

Figure 8. Packing arrangement of *p,p'*-dimethoxybenzophenone viewed in the *ab* plane. A magnetic interaction model of diphenylmethylenes is also shown.

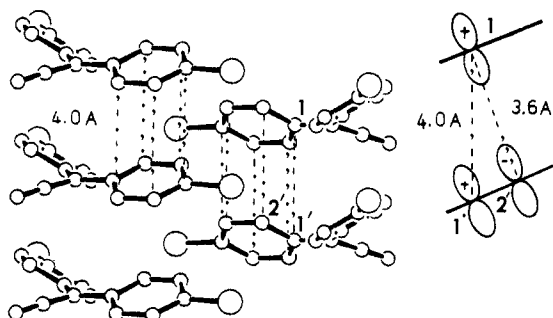


Figure 9. Packing arrangement of **6** viewed along the *a* axis. A schematic side view showing the magnetic interaction between C-1 and C-1', C-2' is also given.

a model for the crystal structure of diazo compound **4** and the generated carbene **2**. The magnetic model discussed above is in accord with the crystal structure. Among four independent molecules in the unit cell one benzene ring of the ketone molecule is nearly in parallel with the benzene ring of an adjacent molecule,

taking pseudo-para type orientation,⁹ although the center of the benzene ring is shifted and only two carbon atoms on the benzene ring are interacting effectively (Figure 8). The molecular orientation satisfies McConnell's theory⁷ in a sense that the carbon atoms with positive spin densities face those with negative ones at the interacting sites. The molecular packing also rationalizes weak interaction between Q pairs. The fact that the zero-field parameters were close to those of pseudo-para-bis(phenylmethylene)[2.2]paracyclophane is consistent with the above model.

The crystal structure of **6** ($P2_1/a$) was revealed by an X-ray analysis. The molecular packing was found to have a layered structure, and benzene rings are overlapped taking pseudo-geminal orientation (Figure 9). Thus antiferromagnetic intermolecular interaction is anticipated between the carbene species based on McConnell's relation, including direct interaction between carbene carbon atoms with the largest spin densities. The interaction however may not be very strong, because the inclination of benzene rings brings the distance, e.g., between C-1 and C-2' (3.6 Å) nearer than that of C-1 and C-1' (4 Å), the former having ferromagnetic interaction. This ferromagnetic interaction may reduce the antiferromagnetic coupling. Therefore, it may not be surprising that the quintet state of the carbene pairs is thermally accessible even at low temperatures.

The intriguing intermolecular magnetic interaction was found within clusters of diphenylmethylene molecules which were generated by irradiation on diamagnetic crystals of diazo molecules. The interaction was revealed to be well-explained by the crystal structure of diazo precursors based on McConnell's theory. The interaction however seems not to be extensive and strong enough to manifest macroscopic ferromagnetic property. Design of molecular assembly of diphenylmethylene derivatives with stronger and wider magnetic interaction is necessary. This is hoped to be achieved by introducing some additional intermolecular forces in order to bind carbene molecules tightly in favorable orientation in condensed phase. The project along this line is in progress in these laboratories.

Acknowledgment. We are indebted to Professor J. Tanaka, Dr. T. Katayama, and A. Kawamoto of Nagoya University for their skillful help in performing the X-ray diffraction analysis of *p,p'*-dichlorodiphenyldiazomethane **6**. We also thank Professor K. Itho, Dr. T. Takui, and Dr. Y. Teki for interpretation of ESR spectra of quintet species.

Fluorescence-Detected Circular Dichroism of Ethidium Bound to Nucleic Acids

Michael L. Lamos, Eric W. Lobenstine, and Douglas H. Turner*

Contribution from the Department of Chemistry and Laboratory for Laser Energetics, University of Rochester, Rochester, New York 14627. Received December 17, 1985

Abstract: Fluorescence-detected circular dichroism (FDCD) spectra of ethidium bound to poly(nucleotides), dinucleotides, tRNA, and DNA are reported. FDCD spectra show bands at approximately 275, 320, and 380 nm. All three bands are sensitive to base sequence at the ethidium binding site. For the bands near 320 and 380 nm, the largest magnitudes are observed for pyrimidine-purine sequences. In addition, the 275-nm band is sensitive to poly(nucleotide) structure near the ethidium binding site, and the 320-nm band is sensitive to spacing between ethidiums. FDCD spectra of ethidium bound to tRNA and DNA are consistent with an intercalative binding site and with a sequence preference for binding. FDCD spectra also indicate that ethidium binding to poly(dA-dG)-poly(dC-dT) is unusual.

Fluorescence-detected circular dichroism (FDCD)¹⁻³ is a spectroscopic technique for monitoring the local environment of

a fluorescent chromophore. FDCD combines the selectivity and sensitivity of fluorescence detection with the conformational

Table I. Summary of Results for Ethidium Bound to Polymers

polymer	FDCD λ_{\max}^a nm (± 5 nm)		av UV CD magnitude, ^b (mdeg ± 1)	av $10^3 g_F$		
	UV	vis		av UV ^c (± 0.2)	at $r = 0.3$, 320 nm ^d (± 0.05)	av vis ^e (± 0.2)
poly(dA-dT)	280	380		0.9	0.96	-4.0
poly(dA)·poly(dT)	270	380	3.0	0.1	-0.01	-2.0
poly(dA-dU)	285	380		1.0	1.34	-3.4
poly(dA)·poly(dU)	275	380	8.7	0.4	0.48	-1.2
poly(A)·poly(U)	275	382	39.6	1.6	0.37	-1.6
poly(dI-dC)	265	380		1.4	1.13	-3.3
poly(dI)·poly(dC)	275	376	-0.5	0.1	0.48	-1.0
poly(I)·poly(C)	279	375	15.9	0.9	0.38	-0.7
poly(dG-dC)	270	388		0.9	0.93	-3.0
poly(G-C)	271	386		1.0	1.00	-2.7
poly(dG)·poly(dC)	263	380	17.9	0.7	0.40	-0.7
poly(dA-dC)·poly(dG-dT)	279	386		0.7	0.98	-2.6
poly(dA-dG)·poly(dC-dT)	260	386	9.3	0.3	0.32	-1.5

^a λ_{\max} was determined from all spectra measured. Any variations were not systematic with r . ^b The transmission CD was averaged over the wavelength interval ± 5 nm from the FDCD λ_{\max} for all r measured. ^c The g_F was averaged over the wavelength interval ± 5 nm from λ_{\max} for all r measured. ^d The g_F was averaged from 310 to 330 nm for $r = 0.3$. ^e The g_F was averaged over the wavelength interval ± 10 nm from λ_{\max} for all r measured.

sensitivity of circular dichroism (CD). It can also be used to measure spectra for highly scattering and/or optically dense samples.⁴⁻⁶ One area where these advantages can be particularly useful is the study of drug binding to macromolecules. If the drug is fluorescent, its CD can be monitored at low concentrations in the presence of other species. Spectra can also be measured in vivo and compared with spectra measured in solution.⁷ Ethidium is a drug that binds to nucleic acids with a concomitant induced CD^{8,9} and enhancement of fluorescence.¹⁰ In this paper, we determine the information available from FDCD spectra of ethidium bound to nucleic acids. Each band of the spectrum is sensitive to different aspects of the binding. These bands are used to provide insights into the binding of ethidium to DNA, transfer RNA, and poly(nucleotides).

Materials and Methods

Sample Preparation. Ethidium bromide was purchased from Sigma and recrystallized from methanol. Poly(nucleotide) and dinucleotide solutions were prepared in a buffer (buffer 1) of 4 mM Na_2HPO_4 , 6 mM NaH_2PO_4 , 1 mM EDTA, and 100 mM NaCl, pH 7.0. Poly(A)·poly(U), poly(I)·poly(C), poly(dG-dC), poly(dA-dC)·poly(dG-dT), poly(dA-dU), poly(dI-dC), and poly(dA-dG)·poly(dC-dT) were purchased from Pharmacia, dissolved in buffer 1, and dialyzed overnight at 4 °C in buffer 1. Poly(dI)·poly(dC) and poly(dA)·poly(dU) were purchased from Pharmacia, dissolved in buffer 1, and heated to 45 °C for 15 min prior to use to assure double strands in solution.¹¹ Poly(dA)·poly(dT), poly(dA-dT), and poly(dG)·poly(dC) were obtained from Sigma, dissolved in buffer 1, and dialyzed overnight at 4 °C in buffer 1. A melting curve was obtained for poly(dG)·poly(dC) to ensure a double stranded form. The melting temperature of 77 °C (in 0.01 M NaCl) was near the 81 °C measured by Inman and Baldwin.¹² Poly(G-C) was a generous gift from Drs. P. Cruz and I. Tinoco, Jr., and was used without further purification.

E. coli, calf thymus, *C. perfringens*, and *M. lysodeikticus* DNA were obtained from Sigma, dissolved in buffer 1, sonicated 30 min, phenol extracted, and dialyzed overnight at 4 °C in buffer 1 prior to use.

The 3'-5' dinucleoside monophosphates were obtained from Sigma, except UpG, which was obtained from Collaborative Research. The dinucleoside monophosphates were dissolved in buffer 1 and used without further purification.

Yeast tRNA^{phe} and E. coli tRNA^{glu2} were purchased from Sigma and dissolved in a buffer (buffer 2) of 4 mM NaH_2PO_4 , 6 mM Na_2HPO_4 , 10 mM MgCl_2 , and 170 mM NaCl, pH 7.0. The tRNAs were dissolved in buffer 2 and dialyzed overnight at 4 °C.

Extinction coefficients were from Bresloff and Crothers¹³ (calf thymus DNA, poly(dI)·poly(dC), poly(I)·poly(C), poly(dI-dC), and poly(A)·poly(U)), Baguley and Falkenhaus¹⁴ (poly(dA-dC)·poly(dG-dT), poly(dA-dG)·poly(dC-dT), and poly(dG)·poly(dC)), Winkle et al.¹⁵ (E. coli, *C. perfringens*, and *M. lysodeikticus* DNA, and ethidium), Handbook of Biochemistry and Molecular Biology¹⁶ (dinucleoside monophosphates), and Bittman¹⁷ (tRNA^{phe} and tRNA^{glu2}). Nucleotide concentrations for polymers varied from 50 to 100 μM (base pairs).

The bound drug to base pair ratio, r , was calculated using the absorbance of ethidium at 480 nm as described by Walker et al.¹⁸ For all polymer solutions, except tRNA, at least 40% of the ethidium was bound. All polymer concentrations are expressed in terms of base pairs, except the tRNA concentrations, which are expressed in terms of nucleotide pairs. Spectra were recorded at ambient temperature (22 °C) except for ethidium-dinucleotide spectra, which were recorded at 2 °C.

FDCD. The FDCD instrument has been described previously.^{7,19} The signal measured is^{2,7}

$$2 \frac{(F_L - F_R)}{(F_L + F_R)} = \frac{2(g_F - 2R)}{(2 - g_F R)} \approx g_F - 2R \quad (1)$$

where

$$R = \frac{A_L(1 - 10^{-A_R}) - A_R(1 - 10^{-A_L})}{A_L(1 - 10^{-A_R}) + A_R(1 - 10^{-A_L})} \quad (2)$$

Here F_L and F_R are fluorescence intensities excited by left and right circularly polarized light, respectively; A_L and A_R are the absorbances of the sample for left and right circularly polarized light, respectively, and are obtained from the CD and absorbance of the sample; g_F is the FDCD dissymmetry factor.²⁰ If all fluorescence is due to absorption by

(1) Abbreviations: FDCD, fluorescence-detected circular dichroism; CD, circular dichroism; DNA, deoxyribonucleic acid; RNA, ribonucleic acid; tRNA, transfer ribonucleic acid; A, adenine; C, cytosine; G, guanine; T, thymine, U, uracil.

(2) Turner, D. H.; Tinoco, I., Jr.; Maestre, M. *J. Am. Chem. Soc.* **1974**, *96*, 4340-4342.

(3) Turner, D. H. *Methods Enzymol.* **1978**, *49G*, 199-214.

(4) White, T. G.; Pao, Y.-H.; Tang, M. M. *J. Am. Chem. Soc.* **1975**, *97*, 4751-4753.

(5) Tinoco, I., Jr.; Turner, D. H. *J. Am. Chem. Soc.* **1976**, *98*, 6453-6456.

(6) Reich, C.; Maestre, M. F.; Edmondson, S.; Gray, D. M. *Biochemistry* **1980**, *19*, 5208-5213.

(7) Lamos, M. L.; Turner, D. H. *Biochemistry* **1985**, *24*, 2819-2822.

(8) Aktipis, S.; Martz, W. W. *Biochem. Biophys. Res. Commun.* **1970**, *39*, 307-313.

(9) Dalgleish, D. G.; Peacocke, A. R.; Fey, G.; Harvey, C. *Biopolymers* **1971**, *10*, 1853-1863.

(10) Lepecq, J.-B.; Paoletti, C. *J. Mol. Biol.* **1967**, *27*, 87-106.

(11) *Pharmacia Molecular Biologicals Catalogue*; Intelligencer Printing Co., 1984; p 113.

(12) Inman, R. B.; Baldwin, R. L. *J. Mol. Biol.* **1964**, *8*, 452-469.

(13) Bresloff, J. L.; Crothers, D. M. *Biochemistry* **1981**, *20*, 3547-3553.

(14) Baguley, B. C.; Falkenhaus, E.-M. *Nucleic Acids Res.* **1978**, *5*, 161-171.

(15) Winkle, S. A.; Rosenberg, L. S.; Krugh, T. R. *Nucleic Acids Res.* **1982**, *10*, 8211-8223.

(16) Fasman, G. D. *Handbook of Biochemistry and Molecular Biology*, 3rd ed.; CRC Press: Boca Raton, FL, 1975; p 597.

(17) Bittman, R. *J. Mol. Biol.* **1969**, *46*, 251-268.

(18) Walker, G. T.; Stone, M. P.; Krugh, T. R. *Biochemistry* **1985**, *24*, 7462-7471.

(19) Lamos, M. L.; Walker, G. T.; Krugh, T. R.; Turner, D. H. *Biochemistry* **1986**, *25*, 687-691.

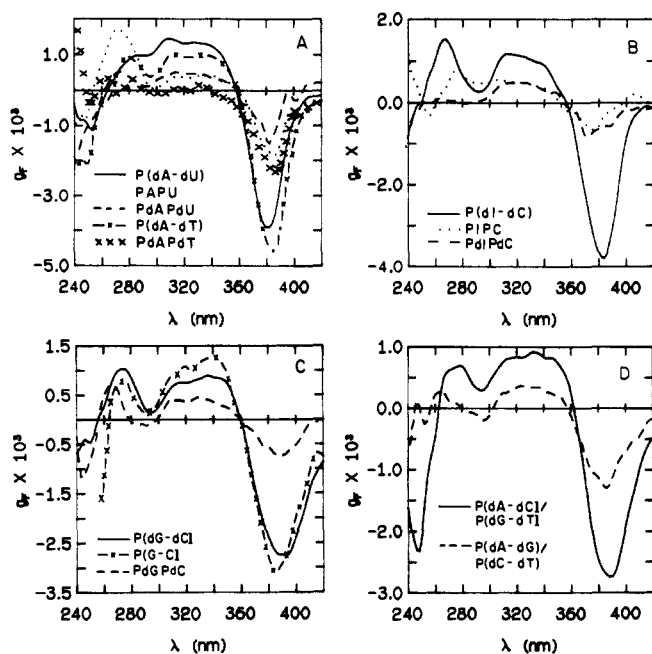


Figure 1. g_F spectra of ethidium binding to (A) poly(dA-dT) (-x-), poly(dA)·poly(dT) (x x x), poly(dA-dU) (—), poly(A)·poly(U) (···), and poly(dA)·poly(dU) (- - -); (B) poly(dI-dC) (—), poly(I)·poly(C) (···), and poly(dI)·poly(dC) (- - -); (C) poly(dG-dC) (—), poly(G-C) (-x-), and poly(dG)·poly(dC) (- - -); (D) poly(dA-dC)·poly(dG-dT) (—) and poly(dA-dG)·poly(dC-dT) (- - -). For all spectra [nucleotide] = 50 μ M, r = 0.3.

one chromophore, then $g_F = \Delta\epsilon_F/\epsilon_F$, the Kuhn dissymmetry factor of the fluorophore, where $\Delta\epsilon_F$ and ϵ_F are the molar CD and absorptivity of the fluorophore, respectively. The g_F were calculated from the FDCD, CD, and absorbance spectra by using the appropriate rearrangement of eq 1. If fluorescence due to several species is detected, then the contribution of each to g_F is weighted by the quantum yield and concentration of each.⁵ For the wavelength range studied, the fluorescence intensity of ethidium increases about 10–60-fold on binding to nucleic acids.²¹ Thus, contributions due to free ethidium should be small. For comparison with previous work, $\theta_F^\circ = -28.65(F_L - F_R)/(F_L + F_R)$, where θ_F° is the FDCD signal in degrees.

FDCD cell path lengths were 1 cm for poly(nucleotide) and tRNA experiments and 2 mm for dinucleoside monophosphate experiments. Filters were Schott GG-10 combined with Corning CS3-66. Separate Pockels cells were used for the 240–350- and 300–420-nm regions in order to increase the lifetime of the Pockels cells.

Other Spectra. CD and absorption spectra were recorded on a Jasco J-40 spectropolarimeter and a Perkin-Elmer 330 spectrophotometer, respectively. Both were interfaced to a PDP-11 computer. Cell path lengths were the same as for the FDCD spectra.

Results

Ethidium Binding to Poly(nucleotides). Figure 1 shows representative g_F spectra for ethidium binding at $r = 0.3$ to poly(dA-dT), poly(dA)·poly(dT), poly(dA-dU), poly(dA)·poly(dU), and poly(A)·poly(U) (Figure 1A); poly(dI-dC), poly(dI)·poly(dC), and poly(I)·poly(C) (Figure 1B); poly(dG-dC), poly(G-C), and poly(dG)·poly(dC) (Figure 1C); and poly(dA-dC)·poly(dG-dT) and poly(dA-dG)·poly(dC-dT) (Figure 1D). The spectra have positive bands near 275 and 320 nm and a negative band near 380 nm. The wavelengths for the maxima near 275 and 380 nm depend on the poly(nucleotide) and are listed in Table I.

The magnitude of the FDCD band near 275 nm remains approximately constant as ethidium is added in the range $r = 0.01$ –0.5, except for poly(dA-dG)·poly(dC-dT) (see Figure 2 and supplementary material). The magnitude of the corresponding transmission CD band also remains approximately constant except for alternating pyrimidine–purine sequences. For the latter, the

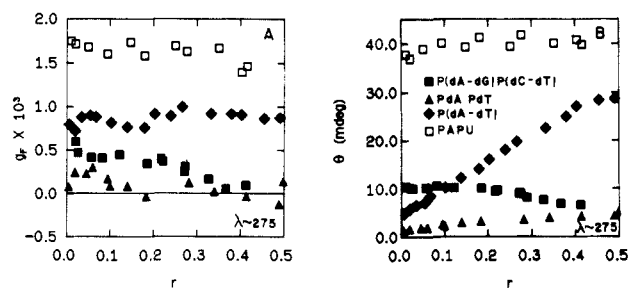


Figure 2. Plots of (A) g_F averaged over the wavelength range indicated vs. r for ethidium binding to poly(dA-dG)·poly(dC-dT) (■, 271 \pm 5 nm), poly(dA)·poly(dT) (▲, 280 \pm 5 nm), poly(dA-dT) (◆, 270 \pm 5 nm), and poly(A)·poly(U) (□, 275 \pm 5 nm); (B) θ vs. r for ethidium binding to poly(dA-dG)·poly(dC-dT) (■, 271 \pm 5 nm), poly(dA)·poly(dT) (▲, 280 \pm 5 nm), poly(dA-dT) (◆, 270 \pm 5 nm), and poly(A)·poly(U) (□, 275 \pm 5 nm).

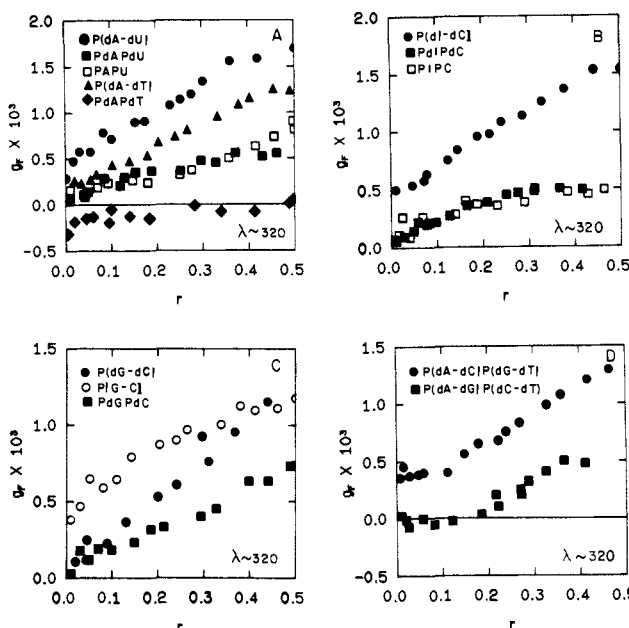


Figure 3. Plots of g_F averaged from 310 to 330 nm vs. r for ethidium binding to (A) poly(dA-dT) (▲), poly(dA)·poly(dT) (◆), poly(dA-dU) (●), poly(A)·poly(U) (□), and poly(dA)·poly(dU) (■); (B) poly(dI-dC) (●), poly(I)·poly(C) (□), and poly(dI)·poly(dC) (■); (C) poly(dG-dC) (●), poly(G-C) (○), and poly(dG)·poly(dC) (■); (D) poly(dA-dC)·poly(dG-dT) (●), poly(dA-dG)·poly(dC-dT) (■).

magnitude increases as r increases (see Figure 2 and supplementary material). The average magnitudes of the relatively constant FDCD and CD bands are listed in Table I. In general, the magnitude of the FDCD band depends on both polymer sequence and whether the ethidium is bound to a deoxyribose or ribose polymer. The FDCD magnitude correlates with the CD in the same wavelength region when pyrimidine–purine sequences are eliminated. At these wavelengths, both ethidium and the nucleic acid bases absorb. Since nucleotides within about four base pairs will transfer energy to ethidium,²² this FDCD band presumably reflects the polymer conformation near the ethidium binding site in addition to the ethidium binding site per se.⁵

As shown in Table I and Figure 3, the magnitude of the band near 320 nm depends on both polymer sequence and the spacing between ethidiums on the polymer. For polymers with alternating pyrimidine–purine sequences, the magnitude of this band is usually 2–3 times larger than for other sequences containing the same base composition. The magnitude of this band also increases as the spacing between ethidiums decreases, in a manner similar to that reported for transmission CD.^{9,23–28} For r values less than

(20) Lobenstine, E. W.; Schaefer, W. C.; Turner, D. H. *J. Am. Chem. Soc.* **1981**, *103*, 4936–4940.

(21) (a) Burns, V. W. F. *Arch. Biochem. Biophys.* **1971**, *145*, 248–254.

(b) Lepecq, J.-B. *Methods Biochem. Anal.* **1971**, *20*, 41–86.

(22) Sutherland, J. C.; Sutherland, B. M. *Biopolymers* **1970**, *9*, 639–653.

(23) Aktipis, S.; Kindelis, A. *Biochemistry* **1973**, *12*, 1213–1221.

(24) Aktipis, S.; Martz, W. W. *Biochemistry* **1974**, *13*, 112–118.

Table II. Summary of Results for Ethidium Bound to Dinucleoside Monophosphates

sequences	$10^{-5}K$		FDCCD λ_{\max} , nm (± 2 nm)		av $10^3 g_F$	
	Dahl et al. (1982), 0 °C	this work, 2 °C	UV	vis	320 nm ^a (± 0.05)	vis ^b (± 0.2)
UpA	7.2 \pm 1.0		275	379	0.59	-1.3
ApU	0.5 \pm 0.1		280	370	0.16	0.0
ApA/UpU	3.0 \pm 0.4		282	385	0.36	0.4
CpG	890 \pm 200	190 \pm 70	260	378	1.05	-3.7
GpC		8.9 \pm 4.5	283	385	-0.05	0.1
GpG/CpC		1.7 \pm 0.6	260	378	0.58	-0.3
CpA/UpG	150 \pm 20		260	381	0.83	-2.2
ApC/GpU		2.0 \pm 0.9	280	375	0.15	0.0
ApG/CpU	4.9 \pm 1.2		260	380	0.32	-0.8
GpA/UpC			285	385	0.12	0.2

^aThe g_F was averaged from 310 to 330 nm. ^bThe g_F was averaged over the wavelength interval ± 10 nm from λ_{\max} .

0.1, poly(dA-dC)·poly(dG-dT) and poly(dA-dG)·poly(dC-dT) are exceptions to this rule. At these low r values, they have magnitudes that are relatively independent of r . Poly(dA)·poly(dT) is also an exception. It has a small, negative magnitude at 320 nm for all values of r . In contrast to the 275-nm band, the magnitude of the 320-nm band is approximately the same for deoxyribose and ribose poly(nucleotides).

As shown in Table I and Figure 4, the magnitude of the band near 380 nm depends on polymer sequence, with alternating pyrimidine-purine sequences having magnitudes 2-4 times larger than other sequences with the same base composition. For both homopolymers and alternating pyrimidine-purine sequences, the magnitude of the 380-nm band follows the same order with base composition: AT > AU > IC > GC. The magnitude of the 380-nm band is relatively independent of whether the polymer has a deoxyribose or ribose backbone and of the ethidium spacing. Exceptions to the latter rule are observed. Magnitudes for poly(dG)·poly(dC) and poly(dA-dG)·poly(dC-dT) decrease continuously with decreasing ethidium spacing. Moreover, below r values of about 0.1, the magnitude at 380 nm decreases slightly with increasing ethidium concentration for poly(dA-dC)·poly(dG-dT) and poly(dA-dG)·poly(dC-dT). These are the same polymers that exhibit anomalous behavior for the 320-nm band in this region of r values.

Ethidium Binding to Dinucleotides. Krugh pioneered the use of dinucleotides as model systems for studying the binding of ethidium to nucleic acids²⁹⁻³² and discovered that ethidium prefers binding to a pyrimidine-purine sequence.³¹⁻³³ Dahl et al.²⁸ reported FDCCD spectra from 230 to 375 nm for ethidium bound to several dinucleotides. FDCCD spectra from 250 to 420 nm for several dinucleotides are reported in Figure 5, and peak positions and magnitudes are reported in Table II. The largest magnitudes for the bands near 320 and 380 nm are observed for pyrimidine-purine sequences. To see if this difference in magnitude is related to a difference in the amount of complexed ethidium, binding constants were determined with the Bines-Hildebrand method.³⁴ These are listed in Table II along with those determined by Dahl et al.²⁸ for slightly different salt conditions. In all cases, over 90% of the ethidium is bound at the concentrations used in the FDCCD experiments.

Ethidium Binding to tRNA. Figure 6 shows representative g_F spectra of ethidium bound to tRNA^{phe} and tRNA^{glu2} at an r of

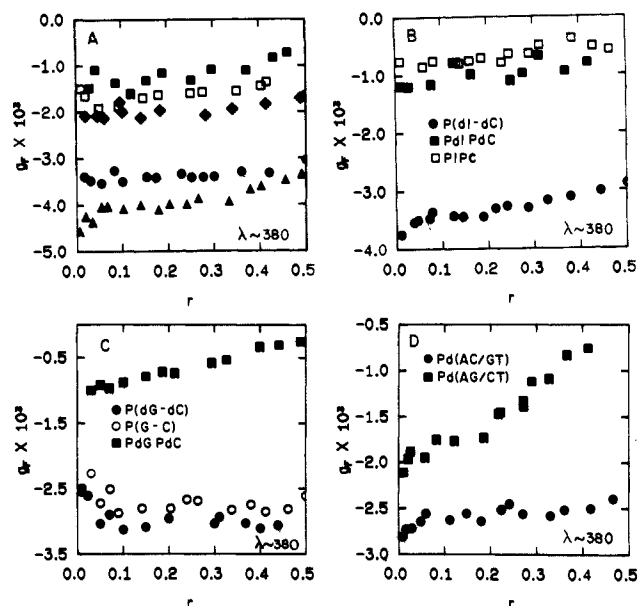


Figure 4. Plots of g_F averaged over the wavelength range indicated vs. r for ethidium binding to (A) poly(dA-dT) (\blacktriangle , 380 ± 10 nm), poly(dA)·poly(dT) (\blacklozenge , 380 ± 10 nm), poly(dA-dU) (\bullet , 380 ± 10 nm), poly(A)·poly(U) (\square , 382 ± 10 nm), and poly(dA)·poly(dU) (\blacksquare , 380 ± 10 nm); (B) poly(dI-dC) (\bullet , 380 ± 10 nm), poly(I)·poly(C) (\square , 375 ± 10 nm), and poly(dI)·poly(dC) (\blacksquare , 376 ± 5 nm); (C) poly(dG-dC) (\bullet , 388 ± 10 nm), poly(G-C) (\circ , 386 ± 10 nm), and poly(dG)·poly(dC) (\blacksquare , 380 ± 10 nm); (D) poly(dA-dC)·poly(dG-dT) (\bullet , 386 ± 10 nm), poly(dA-dG)·poly(dC-dT) (\blacksquare , 386 ± 10 nm).

0.01. The spectra resemble those of poly(A)·poly(U) at $r = 0.05$ and poly(G-C) at $r = 0.01$, respectively. These are also plotted in Figure 6.

Figure 7 shows g_F vs. r for ethidium with tRNA^{phe} and tRNA^{glu2} for the bands near 275, 320, and 380 nm. In contrast to the poly(nucleotides), all three FDCCD bands decrease as r increases. The value of g_F levels off above an r of about 0.04. The decrease in g_F could be due to binding of ethidium at outside binding sites, an increase in unbound ethidium, or a combination of both. In either case, g_F is likely to be lower and would be expected to decrease the FDCCD signal.^{5,19} The magnitudes at 320 and 380 nm for tRNA^{glu2} are consistently larger than for tRNA^{phe}, presumably reflecting a difference in the binding site.

Also shown in Figure 7A is the average magnitude of the transmission CD for tRNA^{phe} and tRNA^{glu2} from 270 to 280 nm. The CD suggests a conformational change occurs between $r = 0.04$ and 0.06. This is the region where the average number of ethidiums bound per tRNA increases from one to two.

Ethidium Binding to Native DNAs. Figure 8 shows representative g_F spectra of ethidium binding at $r = 0.3$ to *M. lysodeikticus*, *E. coli*, calf thymus, and *C. perfringens* DNA. The spectra are similar with a small positive peak at 275 nm, a broad positive band at 320 nm, and a large negative peak at 380 nm. Plots of g_F vs. r for all three bands are shown in Figure 9. For

(25) Houssier, C.; Hardy, B.; Fredericq, E. *Biopolymers* **1974**, *13*, 1141-1160.

(26) Williams, R. E.; Seligy, V. L. *Can. J. Biochem.* **1974**, *52*, 281-287.

(27) Parodi, S.; Kendall, F.; Nicolini, C. *Nucleic Acids Res.* **1975**, *2*, 477-486.

(28) Dahl, K. S.; Pardi, A.; Tinoco, I., Jr. *Biochemistry* **1982**, *21*, 2730-2737.

(29) Krugh, T. R. *Proc. Natl. Acad. Sci. U.S.A.* **1972**, *69*, 1911-1914.

(30) Krugh, T. R.; Neely, J. W. *Biochemistry* **1973**, *12*, 1775-1782.

(31) Krugh, T. R.; Reinhardt, C. G. *J. Mol. Biol.* **1975**, *97*, 133-162.

(32) Krugh, T. R.; Wittlin, F. N.; Cramer, S. P. *Biopolymers* **1975**, *14*, 197-210.

(33) Reinhardt, C. G.; Krugh, T. R. *Biochemistry* **1978**, *17*, 4845-4854.

(34) Benesi, H. A.; Hildebrand, J. H. *J. Am. Chem. Soc.* **1949**, *71*, 2703-2707.

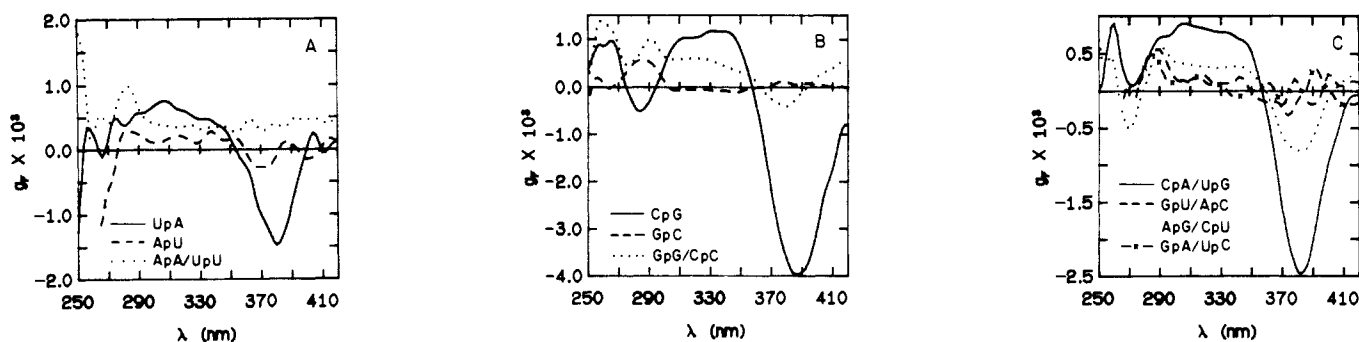


Figure 5. FDCD spectra of ethidium with (A) UpA (—), ApU (---), and ApA/UpU (···); (B) CpG (—), GpC (---), and CpC/GpG (···); (C) CpA/UpG (—), GpU/ApC (---), ApG/CpU (···), and GpA/UpC (-·-·). For all spectra [ethidium] = 2×10^{-4} M, total [dinucleotide] = 6×10^{-3} M.

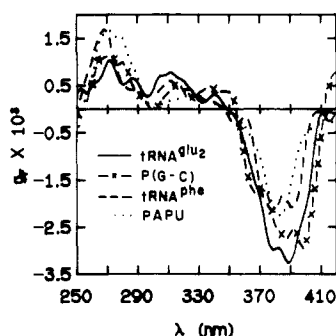


Figure 6. FDCD spectra of ethidium with tRNA^{Glu} (—) at $r = 0.011$, poly(G-C) (-·-·) at $r = 0.01$, tRNA^{Phe} (---) at $r = 0.011$, and poly(A)-poly(U) (···) at $r = 0.05$. [tRNA] = 7.5×10^{-5} M.

the 275-nm band, g_F is relatively constant. For the 320-nm band, g_F increases with increasing r , as it does for most of the other poly(nucleotides). For the 380-nm band, g_F decreases with increasing r . This contrasts with the relatively constant g_F observed near 380 nm for most of the other poly(nucleotides).

Winkle et al.¹⁵ have used phase partition and direct absorption techniques to show that ethidium binds cooperatively to *E. coli* DNA but noncooperatively to calf thymus, *C. perfringens*, and *M. lysodeikticus* DNA. We have repeated the absorption experiments with *E. coli* and calf thymus DNA using absorption spectroscopy under conditions used for obtaining the data shown in Figures 8 and 9 (see Materials and Methods). Our Scatchard plots (see supplementary material) agree with those of Winkle et al.,¹⁵ with *E. coli* DNA exhibiting a positive slope at r values below 0.07 and a negative slope above $r = 0.07$, whereas calf thymus DNA exhibits a negative slope for all r values.

Discussion

FDCD spectra of ethidium bound to nucleic acids exhibit bands near 275, 320, and 380 nm. The 320- and 380-nm bands have been observed previously in transmission CD.^{9,23,25,28} The band near 380 nm, however, has not been studied in detail by transmission CD because it has a small $\Delta\epsilon$ and ϵ . This band is greatly enhanced in FDCD which is sensitive to $\Delta\epsilon/\epsilon$. Thus it can now be studied conveniently. Each FDCD band is sensitive to different aspects of the binding. In this discussion, empirical rules for this sensitivity are presented first, then exceptions to the rules, and finally applications of the rules to provide insights into the binding of ethidium to tRNA and DNA.

Empirical Rules. Whether the polymer has a deoxyribose or ribose backbone affects the magnitude of the band near 275 nm but not the bands near 320 and 380 nm. Since nucleic acid bases absorb at 275 nm, the results suggest energy transfer from nucleic acid bases contributes to the 275-nm band, so that it is probably sensitive to the polymer conformation roughly four base pairs on either side of the ethidium binding site.²² Nucleic acid bases do not absorb above 310 nm, so the 320- and 380-nm bands contain no contribution from base to ethidium energy transfer. Thus they are presumably sensitive to the conformation immediately around the ethidium. Crystal structures of ethidium bound to ribodi-

nucleotide minihelices show a C2'(endo)-C3'(endo) mixed sugar pucker at the binding site.³⁵⁻³⁷ This led Sobell et al.³⁷ to propose that the geometry of the binding site is the same in deoxyribose and ribose polymers. NMR results of Patel and Shen indicate similar mixed sugar pucker for the complexes of propidium with the dimers deoxy- and ribocytidylylguanosine in solution.³⁸ The observation that the FDCD bands at 320 and 380 nm are similar for ethidium bound to deoxyribose and ribose poly(nucleotides) with the same sequence supports the prediction of equivalent geometries in polymers.

The average spacing between ethidiums affects the magnitude of the 320-nm band. This same trend has been observed with transmission CD.^{9,23,25,28} Aktipis and Kindelis²³ and Houssier et al.²⁵ attribute this trend to ethidium-ethidium interactions. Dahl et al.,²⁸ however, noticed that large CD magnitudes are induced at 320 nm when ethidium binds to dinucleotides and attribute the trend to ethidium-induced conformational changes. Our results do not rule out either of these possibilities, and both may make contributions. It is clear, however, that the magnitude of this band can be used to provide information on the spacing between ethidiums intercalated in a polymer. An application of this rule to study the binding of ethidium to left-handed (*Z*-form) poly(nucleotides) has recently been reported.¹⁹

The sequence at the binding site affects the magnitude of the bands near 275, 320, and 380 nm and the wavelength maximum of the bands near 275 and 380 nm. Polymers with alternating pyrimidine-purine sequences have the largest magnitudes for the bands at 320 and 380 nm. These polymers have equal numbers of pyrimidine-purine and purine-pyrimidine binding sites, so this data does not indicate whether one or both sites are associated with the large FDCD magnitudes. The fact that the magnitude of the 380-nm band is relatively independent of r , however, indicates the FDCD is associated with only one of the two possible sites. Alternatively, the binding constants or FDCD of both sites must be similar. It would be surprising if this was true in all six cases studied. The spectra for ethidium bound to the pyrimidine-purine dimers, CpG, UpA, and CpA/UpG, are much different from the spectra for the corresponding purine-pyrimidine dimers, GpC, ApU, and ApC/GpU, but similar to spectra for polymers with the corresponding sequences (see Figures 1 and 5). This suggests the large magnitudes are associated with the pyrimidine-purine sequences. Krugh and co-workers have shown that ethidium binds preferentially to pyrimidine-purine dinucleotides,^{31,32} and the binding constants listed in Table II quantify this.²⁸ The large binding constants and FDCD magnitudes may have a similar origin. The overlap of the nucleic acid bases with ethidium is much larger for pyrimidine-purine than for purine-pyrimidine sequences.^{32,35,36} This difference in stacking could produce the difference in binding constants and also result

(35) Tsai, C. C.; Jain, S. C.; Sobell, H. M. *J. Mol. Biol.* **1977**, *114*, 301-315.

(36) Jain, S. C.; Tsai, C. C.; Sobell, H. M. *J. Mol. Biol.* **1977**, *114*, 317-331.

(37) Sobell, H. M.; Tsai, C. C.; Jain, S. C.; Gilbert, S. G. *J. Mol. Biol.* **1977**, *114*, 333-365.

(38) Patel, D. J.; Shen, C. *Proc. Natl. Acad. Sci. U.S.A.* **1978**, *2553*-2557.

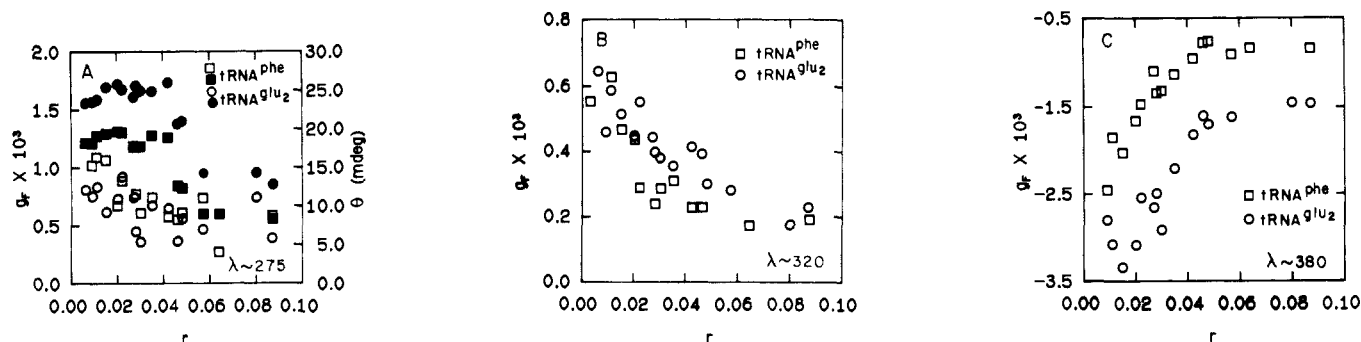


Figure 7. Plots of g_F (open symbols) and θ (filled symbols) averaged over the wavelength range indicated vs. r for ethidium binding to tRNA^{phe} (\square) and tRNA^{glu2} (\circ) at 275 \pm 5 nm (A), 320 \pm 10 nm (B), and 380 \pm 10 nm (C).

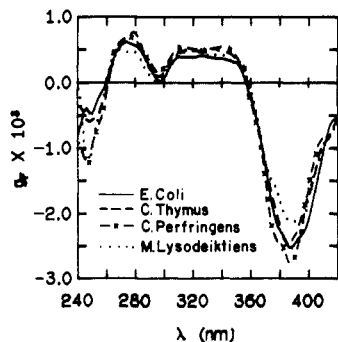


Figure 8. g_F spectra of ethidium with *E. coli* (—), calf thymus (---), *M. lysodeikticus* (···), and *C. perfringens* (-·-·) DNA at $r = 0.3$.

in greater coupling of base and ethidium transition moments to give enhanced optical activity. The latter hypothesis can be tested by calculating with available methods the CD spectra of ethidium bound to various sequences.

Exception to Rules. The FDCD and CD spectra for ethidium bound to poly(dA-dG)·poly(dC-dT) depend on r in unique ways, as shown in Figures 2 and 4. Near 275 nm, g_F is roughly constant until $r = 0.2$ and then decreases as r increases (Figure 2A). Similar behavior is also observed for the transmission CD near 275 nm. Near 320 nm, g_F is essentially zero until $r = 0.2$ and at higher r increases in a manner similar to that observed with other polymers. Near 380 nm, g_F is approximately constant until $r = 0.2$ and then decreases as r increases. Thus all three bands are anomalous, suggesting the binding of ethidium to poly(dA-dG)·poly(dC-dT) is unusual. Perhaps the polymer undergoes a conformational change above $r = 0.2$. X-ray diffraction studies on fibers of poly(dA-dG)·poly(dC-dT) indicate it is unable to adopt an A-form conformation.³⁹ This suggests it is very unfavorable for this polymer to have a C3'(endo) sugar conformation, and this may be related to its unusual behavior in binding ethidium. More detailed experiments using other techniques are required to further characterize this binding.

The FDCD band near 320 nm behaves somewhat unusually for ethidium bound to poly(dA-dC)·poly(dG-dT) and poly(dA)·poly(dT). With poly(dA-dC)·poly(dG-dT), the magnitude of the 320-nm band is apparently constant until $r = 0.1$. Such behavior has been previously observed by both transmission CD and FDCD for ethidium binding to poly(dG-dC) in 4.4 M NaCl and interpreted as indicating clustering of ethidium.^{18,19} By analogy, the results suggest ethidium may initially bind to poly(dA-dC)·poly(dG-dT) by clustering roughly 10 base pairs apart. With poly(dA)·poly(dT), the 320-nm band has a small negative magnitude for all values of r , and the 275-nm band is also small. This suggests little interaction between bound ethidiums and between ethidium and nucleic acid bases. This behavior may again reflect unusual binding to this polymer. This is not surprising since several previous studies indicate poly(dA)·poly(dT) has

unusual conformational and drug binding properties.^{13,40,41}

An unusual FDCD spectrum is also observed for ethidium bound to ApA/UpU. In particular, above 300 nm a very broad, positive band is observed (see Figure 5). This contrasts with the negative peak near 382 nm in the spectrum of poly(A)-poly(U) (see Figure 1). Absorption measurements indicate ethidium is binding to the dimers in a 1:1:1 complex (see Table II and Dahl et al.²⁸). Evidently, the geometries of the complexes with dimers and polymers are markedly different. CD measurements have previously shown that the geometries of single stranded ApA and poly(A) are also different.⁴² The results indicate dimers are not always good model systems for binding of drugs to polymers.

Ethidium Binding to tRNA. Based on X-ray diffraction data, Leibman et al.⁴³ propose ethidium binds to yeast tRNA^{phe} without intercalation. Based on NMR data, however, Jones et al.^{44,45} propose ethidium binds to yeast tRNA^{phe} by intercalation between the base pairs formed by the sequences U6-U7 and A66-A67, and to *E. coli* tRNA^{glu2} by intercalation next to at least one GC base pair. The FDCD spectra of ethidium bound to tRNA support this intercalative binding model.

It has been shown previously that the 320- and 380-nm FDCD bands are absent when ethidium binds to single stranded poly(U), liver glutamate dehydrogenase, poly(L-glutamic acid), and (carboxymethyl)cellulose.⁷ None of these molecules permit intercalative binding. These bands are present, however, in the FDCD spectra of ethidium bound to double helical nucleic acids where binding is by intercalation (see Figures 1, 5, and 8). Thus the presence of these bands in the FDCD spectra for ethidium bound to tRNA^{phe} and tRNA^{glu2} is consistent with intercalation.

As shown in Figure 7, the magnitudes of the FDCD bands decrease as ethidium is added to tRNA. This is opposite the trend observed with poly(nucleotides). Equilibrium studies indicate there is one strong binding site for ethidium on tRNA under salt conditions corresponding to those for Figure 7.⁴⁶⁻⁴⁸ Additional ethidiums will either remain free in solution or bind weakly in an outside complex.^{17,49,50} These additional ethidiums have either zero or small FDCD magnitudes, thereby reducing the overall magnitude measured.⁵ Thus the magnitudes of the FDCD bands are consistent with a single strong ethidium binding site.

(40) Arnott, S.; Chandrasekaran, R.; Hall, I. H.; Puigjaner, L. C. *Nucleic Acids Res.* **1983**, *11*, 4141-4155.

(41) Wilson, W. D.; Wang, Y.-H.; Krishnamoorthy, C. R.; Smith, J. C. *Biochemistry* **1985**, *24*, 3991-3999.

(42) Causley, G. C.; Johnson, W. C., Jr. *Biopolymers* **1983**, *22*, 945-967.

(43) Leibman, M.; Rubin, J.; Sundaralingam, M. *Proc. Natl. Acad. Sci. U.S.A.* **1977**, *74*, 4821-4825.

(44) Jones, C. R.; Kearns, D. R. *Biochemistry* **1975**, *14*, 2660-2665.

(45) Jones, C. R.; Bolton, P. H.; Kearns, D. R. *Biochemistry* **1978**, *17*, 601-607.

(46) Tao, T.; Nelson, J. H.; Cantor, C. R. *Biochemistry* **1970**, *9*, 3514-3524.

(47) Urbanke, C.; Romer, R.; Maass, G. *Eur. J. Biochem.* **1973**, *33*, 511-516.

(48) Sakai, T. T.; Torget, R. I. J.; Freda, C. E.; Cohen, S. S. *Nucleic Acids Res.* **1975**, *2*, 1005-1022.

(49) Tritton, T. R.; Mohr, S. C. *Biochem. Biophys. Res. Commun.* **1971**, *45*, 1240-1249.

(50) Tritton, T. R.; Mohr, S. C. *Biochemistry* **1973**, *12*, 905-914.

(39) Leslie, A. G. W.; Arnott, S.; Rengaswami, C.; Ratliff, R. L. *J. Mol. Biol.* **1980**, *143*, 49-72.

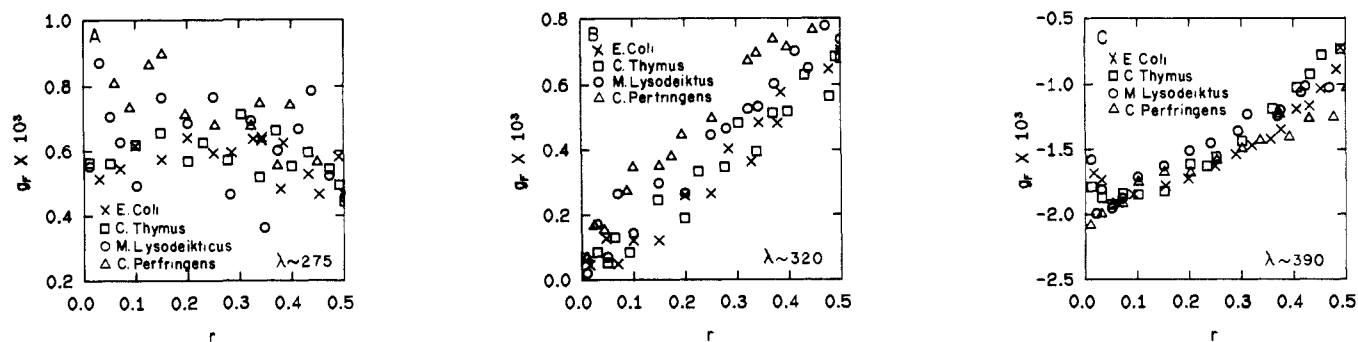


Figure 9. Plots of g_F averaged over the wavelength range indicated vs. r for ethidium binding to *E. coli* (X), calf thymus (□), *M. lysodeikticus* (O), and *C. perfringens* (Δ) DNA for data at (A) 275 ± 5 nm, (B) 320 ± 5 nm, and (C) 386 ± 10 nm.

Jones et al.⁴⁵ suggest the strong ethidium binding site in tRNA^{phe} is between the base pairs formed by U6–U7 and A66–A67 or A5–U6 and A67–U68. If the former site is preferred, then the FDCD spectrum above 300 nm would resemble that measured for poly(A)·poly(U). As shown in Figure 6, the two spectra are very similar. The magnitude of the 380-nm band for tRNA^{glu} is larger than for tRNA^{phe}. This larger magnitude suggests ethidium is intercalated at a pyrimidine–purine sequence. The only such sequence in tRNA^{glu} is between the base pairs formed by C29–G30 and C42–G43. This site is only one base pair away from one of the possible sites suggested by Jones et al.⁴⁵ As shown in Figure 6, the FDCD spectra of ethidium bound to tRNA^{glu} and poly(G–C) are similar. Thus the FDCD spectra are consistent with the conclusions of Jones et al.⁴⁵ and suggest ethidium binds in the anticodon stem of *E. coli* tRNA^{glu}.

Ethidium Binding to DNA. The magnitude of the FDCD band near 380 nm generally decreases as ethidium is added to DNA (see Figure 9C). This trend has been observed previously by transmission CD and attributed to increasing overlap with the positive band below 350 nm.^{23,24} For the poly(nucleotides) shown in Figures 1–4, however, this band remains essentially constant as r increases, which is not consistent with the above interpretation. The data are consistent with a model in which ethidium binds preferentially to pyrimidine–purine sequences at low r , giving large FDCD magnitudes. At higher r , all pyrimidine–purine sites are filled and binding is to sequences that have lower FDCD magnitudes. Thus this evidence suggests the pyrimidine–purine binding preference observed for dinucleotides is also valid for poly(nucleotides). A decrease in magnitude near 380 nm with increasing ethidium concentration has also been observed for FDCD spectra of ethidium taken up by *E. coli* cells.⁷ This suggests there is also a sequence preference *in vivo*. However, experiments *in vivo* must be extended to lower ethidium concentrations to prove this suggestion.

Ethidium binds cooperatively to *E. coli* DNA, but noncooperatively to calf thymus, *C. perfringens*, and *M. lysodeikticus* DNA.¹⁵ As shown in Figure 9, however, there is no significant difference between these DNAs in the way FDCD spectra of bound ethidium change with added ethidium. This indicates the cooperative binding is not associated with a different conformation at the binding site or close clustering of ethidium at low r . Clustering would result in an anomalously high magnitude at low r for the 320-nm FDCD band.^{7,18}

Conclusion

This paper demonstrates several advantages of FDCD for studies of drug binding. The technique can be applied to simple

and complicated, including *in vivo*,⁷ systems. Thus it can provide a spectroscopic test for extrapolations of results from model systems. In the case of ethidium, FDCD spectra indicate that pyrimidine–purine dimers are good models for pyrimidine–purine polymers and that the pyrimidine–purine sequence preference observed for dimers³¹ is also valid for natural DNA. In contrast, ApA/UpU is not a good model for poly(A)·poly(U).

Each band in an FDCD spectrum can be sensitive to different aspects of drug binding. Thus the information content is higher than for circular polarization of luminescence, in which only one band is typically observed.^{51,52} In principle, bands in other spectral regions can be observed for ethidium, increasing the information content further. For example, bands in the vacuum ultraviolet are likely to be especially sensitive to nucleic acid conformation.^{53,54} Presumably these advantages will be useful for studies of other fluorescent ligands.

Acknowledgment. We thank Drs. I. Tinoco, Jr., and P. Cruz for providing poly(G–C), Dr. S. M. Freier for encouragement and helpful discussions, and Drs. T. R. Krugh and C. G. Reinhardt for helpful comments on the manuscript. This work was supported by the National Institutes of Health Grant GM28533.

Registry No. UpA, 3256-24-4; ApU, 3051-84-1; ApA, 2391-46-0; UpU, 2415-43-2; CpG, 2382-65-2; GpC, 4785-04-0; CpC, 2536-99-4; GpG, 3353-33-1; CpA, 2382-66-3; UpG, 3474-04-2; GpU, 4785-07-3; ApC, 4833-63-0; ApG, 3352-23-6; CpU, 2382-64-1; GpA, 6554-00-3; UpC, 3013-97-6; poly(dA–dT)·poly(dA–dT), 26966-61-0; poly(dA)·poly(dT), 24939-09-1; poly(dA–dU)·poly(dA–dU), 34607-75-5; poly(A)·poly(U), 24936-38-7; poly(dA)·poly(dU), 25822-93-9; poly(dI–dC)·poly(dI–dC), 34639-43-5; poly(I)·poly(C), 24939-03-5; poly(dI)·poly(dC), 25853-45-6; poly(dG–dC)·poly(dG–dC), 36786-90-0; poly(G–C)·poly(G–C), 49846-05-1; poly(dG)·poly(dC), 25512-84-9; poly(dA–dC)·poly(dG–dT), 55684-99-6; poly(dA–dG)·poly(dC–dT), 53232-17-0; ethidium bromide, 1239-45-8.

Supplementary Material Available: Plots of g_F vs. r and θ vs. r for poly(nucleotides) and Scatchard plots of ethidium with *E. coli* and calf thymus DNA (3 pages). Ordering information is given on any current masthead page.

(51) Steinberg, I. *Biochemical Fluorescence: Concepts*; Chen, R. F., Ed.; Wiley: New York, 1975; Vol. 1, Chapter 3.

(52) Richardson, F. S.; Riehl, J. P. *Chem. Rev.* **1977**, *77*, 773–792.

(53) Sutherland, J. C.; Griffin, K. P.; Keck, P. C.; Takacs, P. Z. *Proc. Natl. Acad. Sci. U.S.A.* **1981**, *78*, 4801–4804.

(54) Johnson, W. C. Jr. *Methods of Biochemical Analysis*; Glick, D., Ed.; Wiley: New York, 1985; Vol. 31, pp 61–163.